

Heat capacities of polyethylene and linear aliphatic polyoxides

Janusz Grębowicz, Hidematsu Suzuki and Bernhard Wunderlich

Department of Chemistry, Rensselaer Polytechnic Institute, Troy, NY 12181, USA

(Received February 21, 1984)

Heat capacities at constant pressure and volume are calculated from full and partially approximated normal mode frequency spectra for crystalline polyethylene, poly(oxyethylene), poly(oxyethylene), poly(oxytrimethylene), poly(oxytetramethylene), poly(oxyoctamethylene), poly(oxyethyleneoxyethylene), and poly(oxyethyleneoxytetramethylene). A calculation scheme using a Tarasov-function for $2N$ skeletal modes and approximation of the residual normal modes from known data on polyethylene and poly(oxyethylene) is developed for all homologous, linear, aliphatic polyoxides. N is the number of CH_2 -groups in the repeating unit. Calculations can be carried out over the whole temperature range 0 K to melting. For θ -temperatures and constant A_0 for the C_v - to $-C_p$ conversion, oxygen-concentration dependent curves are given. Recommended experimental data bank heat capacities agree to $\pm 5\%$ or better.

(Keywords: crystalline; glassy; heat capacity; polyoxides; polyethylene; vibration spectrum)

INTRODUCTION

The linking of heat capacities of solids of linear macromolecules to their vibrational spectrum¹ has been of long standing interest at ATHAS, our laboratory for Advanced THERmal Analysis². Recently, a complete critical analysis of all measured heat capacities of linear macromolecules has been published in form of a data bank³. Based on this data bank we have tried to interpret the heat capacities, develop predictive capabilities, and explore the limits of our understanding of the theory of heat capacities of linear macromolecules. Work has already been completed on polypropylene⁴ and poly(tetrafluoroethylene)⁵. The present paper contains an update for polyethylene¹. Next, a more detailed analysis of poly(oxyethylene) is attempted. Then, the experimental heat capacities of poly(oxyethylene), poly(oxytrimethylene) and poly(oxytetramethylene) are compared to heat capacity estimates based on the two parent polymers polyethylene and poly(oxyethylene). Based on these five homologous macromolecules, a prediction scheme based on skeletal and group vibration frequencies is developed for the whole homologous series and tested on limited experimental data on poly(oxyoctamethylene), poly(oxyethylene-oxyethylene) and poly(oxyethylene-oxytetramethylene).

The model used for the interpretation of the heat capacity makes use of an approximate separation of the vibrational spectrum into group and skeletal vibrations⁶. Analogous group vibrations change only little from molecule to molecule, as is known also from infra-red and Raman spectroscopy. In our case, the group vibrations involve mainly C-H stretching and bending, and C-C and C-O stretching. The C-H vibrations remain largely decoupled from the skeletal vibrations because of the low H-mass and the correspondingly high frequency. The rather limited coupling of the C-C and C-O stretching vibrations along the chain finds its explanation in the bond

angle which is not far from 90° . This separation of the group vibrations leaves two skeletal vibration modes per chain atom. Efforts to use calculated skeletal vibrations for the heat capacity calculation have not been successful because of difficulties of proper assignment of intermolecular interactions. For heat capacity calculations it is, instead, usually sufficient to use the 3-dimensional Debye function to characterize the rather small number of long wavelength, intermolecular skeletal vibrations. The remaining intramolecular skeletal vibrations are then approximated by a box-distribution as first proposed by Tarasov⁷. The ratio of the number of vibrations described by the 3-dimensional Debye function to the number of vibrations described by the box-distribution is fixed in the Tarasov-treatment by the ratio of the limiting vibration frequencies θ_3/θ_1 . θ_3 and θ_1 are the three- and one-dimensional Debye temperatures, respectively. To have a uniform frequency unit throughout the discussion, all frequencies are quoted in terms of θ -temperatures ($\theta = h\nu/k$, $1 \text{ K} = 2.08 \cdot 10^{10} \text{ Hz}$, $1 \text{ K} = 0.695 \text{ cm}^{-1}$). A full set of inversion routines for low temperature heat capacities corrected for group vibrations to θ_3 and θ_1 has been developed earlier⁸ for our ATHAS computation centre. Similarly, the computation programs for heat capacities from θ_3 , θ_1 and group vibration frequencies have been published before⁹.

The heat capacity contributions of the group vibrations are calculated using Einstein functions for single frequencies, θ_E and box distributions θ_L to θ_U . For the C_p - C_v conversion, the Nernst-Lindemann treatment with A_0 -parameters fitted at 300 K to experimental data on expansivity, α , and compressibility, β , are used¹⁰. The equations are summarized below.

1. Einstein function

$$E(\theta_E/T) = C_v/NR = (\theta_E/T)^2 \exp(\theta_E/T) / [\exp(\theta_E/T) - 1]^2 \quad (1)$$

2. One-dimensional Debye function

$$D_1(\theta_1/T) = C_v/NR = (2T/\theta_1) \int_0^{\theta_1/T} \frac{x^2 dx}{\exp x - 1} - \frac{\theta_1/T}{\exp(\theta_1/T) - 1} \quad (2)$$

3. Three-dimensional Debye function

$$D_3(\theta_3/T) = C_v/NR = (12T^3/\theta_3^3) \int_0^{\theta_3/T} \frac{x^3 dx}{\exp x - 1} - \frac{3\theta_3/T}{\exp(\theta_3/T) - 1} \quad (3)$$

4. Box distribution

$$B(\theta_U/T, \theta_V/T) = C_v/NR = \theta_U/(\theta_U - \theta_V) [D_1(\theta_U/T) - (\theta_U/\theta_V) D_1(\theta_V/T)] \quad (4)$$

5. Tarasov function

$$T(\theta_3/T, \theta_1/T) = C_v/NR = D_1(\theta_1/T) - (\theta_3/\theta_1) [D_1(\theta_3/T) - D_3(\theta_3/T)] \quad (5)$$

6. Nernst-Lindemann equation

$$C_p - C_v = A_0 C_p^2 T/T_m \quad (6)$$

7. Experimental $C_p - C_v$ conversion

$$C_p - C_v = TV\alpha^2/\beta \quad (7)$$

where N is the number of vibrators under consideration and R is the gas constant 8.314 J/(K mol).

Table 1 Vibrations of crystalline, orthorhombic polyethylene*

	Vibration type	N	θ_E or θ_L and θ_U (K)
A. Group Vibrations:			
ν_6	CH ₂ asym. stretch	1	4148.1
ν_1	CH ₂ symmetric stretch	1	4097.7
ν_2	CH ₂ scissoring	1	2074.7
ν_3	CH ₂ wagging	0.65 0.35	1698.3–1976.6 1976.6
ν_7	CH ₂ twisting and rocking	0.48 0.52	1689.6–1874.3 1874.3
ν_4	C–C stretching	0.34 0.35 0.31	1377.6–1637.5 1377.6–1525.4 1525.4
ν_8	CH ₂ rocking and twisting	0.04 0.59 0.37	1494.1 1038.0–1494.1 1079.1
B. Skeletal Vibrations:			
ν_5 and ν_9	C–C–C bending and rotation	0.12 0.42 0.23 0.15 0.32 0.47 0.18 0.06	790.4 138.4–790.4 148.4–790.4 291.8 178.1–291.8 0.1–291.8 138.5 0.1–178.1

*Data fitted to the dispersion curves of ref. 11

POLYETHYLENE

Both, the experimental heat capacities and the vibrational spectrum of polyethylene have seen improvements over the last 20 years, although no major revisions of the earlier analysis¹ is necessary. The present recommended experimental heat capacity of fully crystalline polyethylene³ is based on 45 separate investigations on widely different, usually multiple samples; this contrasts the earlier analysis which could only be based on the five investigations published by 1962. Heat capacities on samples of crystallinities between 0.42 and 0.97 were used to establish C_p for fully crystalline polyethylene³. The heat capacities below 150 K were inverted to the skeletal theta temperatures $\theta_3 = 158$ K and $\theta_1 = 519$ K ($N=2$) after subtraction of the group vibration contributions to the heat capacity⁸. The vibrational spectrum of crystalline, orthorhombic polyethylene has also been critically reviewed recently¹¹. In *Table 1* the vibration frequencies are listed. They correspond closely to the spectrum recommended in ref. 11. The minor splitting due to the two CH₂-chains in the orthorhombic crystal has been averaged where necessary, so that N in *Table 1* refers to one CH₂-unit. The conversion of C_v calculated from the data of *Table 1* to C_p was made using equation (6) with an A_0 -value of $4.85 \cdot 10^{-3}$ (K mol) J⁻¹. This value was derived from a survey of PVT-data by Arora¹² and agrees at room temperature closely to a prior analysis of ours¹³.

Figure 1 displays the results and *Figure 2* the deviations from the experimental recommended data. An attempt to fit the full vibrational spectrum shows major deviations in the very low temperature region. At 1 K the calculated C_p is 473 times too large, at 10 K 4.5 times, and at 20 K it is still 60% larger than the experimental C_p . The extraordinarily high low temperature heat capacities are then compensated by the lower data in the 100 to 250 K region (maximum deviation -4.6%). A similarly poor fit of a calculated spectrum at the lowest temperatures was reported for crystals of poly(tetrafluoroethylene)⁵. It rests with the difficulties in properly assigning intermolecular force constants. The second calculated curve in *Figures 1* and *2* makes use of an experimental fit of the two Tarasov parameters θ_3 and θ_1 (equation (5)) and shows over the

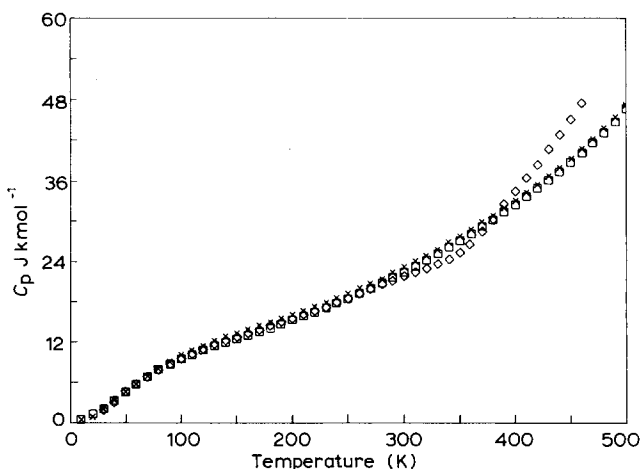


Figure 1 Heat capacity of PE at constant pressure for polyethylene (CH₂)_x. (◇) Recommended experimental data; (□) calculated using all frequencies of *Table 1*; (×) calculated using the group vibrations of *Table 1* and $\theta_3 = 158$ K and $\theta_1 = 519$ K for 2 skeletal vibrations

whole reliable experimental range, 0 to 450 K in steps of 10 K, an average deviation of $1.6 \pm 4.9\%$ which is within the experimental accuracy, although the systematic positive and negative deviations in the 300 and 450 K regions, respectively, are in need of explanation. The prior calculations making use of the work of Tasumi *et al.*¹⁴, who calculated the vibrational frequency spectrum of the

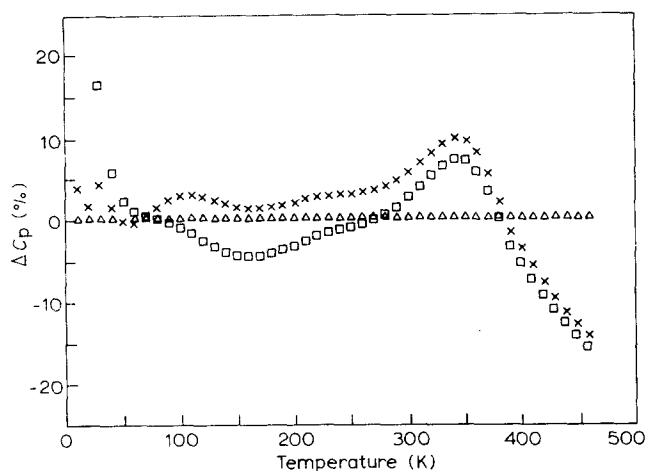


Figure 2 Deviation of the calculated heat capacities C_p of PE from experimental values. (Symbols as in Figure 1). Δ , experimental data

isolated polyethylene chain, deviates from the here presented data by less than 0.5% in heat capacity when replacing ν_5 and ν_9 by the same θ_3 and θ_1 Tarasov treatment. The C_v -data are listed in the general comparison Table 3 below.

POLY(OXYMETHYLENE)

The recommended experimental heat capacities of fully crystalline, trigonal poly(oxyethylene) of the data bank³ range from 0.4 to 390 K. They represent the critically evaluated average heat capacity measurements of four samples of high crystallinity in temperature regions of little or no crystallinity dependence of C_p and 2 samples of full crystallinity. The data were generated in five different laboratories and represent a considerable improvement over the preliminary data of ref. 6. The vibrational spectrum of poly(oxyethylene) was calculated for orthorhombic^{15,16} and trigonal crystals¹⁷. Since over wide temperature ranges heat capacities even of glassy and crystalline macromolecules do not differ much, both frequency spectra were used for the analysis of the heat capacity. The dispersion curves were broken down into the box distributions and single frequencies listed in Table 2. As in the polyethylene case, the splitting of the orthorhombic frequencies was incorporated into the Table

Table 2 Vibrations of crystalline trigonal^a and orthorhombic^b poly(oxyethylene)

Vibration Type	N	Trigonal		Orthorhombic ^b	
		θ_E or θ_L and θ_U (K)	N	θ_E or θ_L and θ_U (K)	
A. Group Vibrations					
ν_1 CH ₂ symmetric stretch	1.0	4284.7	(1.0	4284.7) ^c	
ν_2 CH ₂ asymm. stretch	1.0	4168.2	(1.0	4168.2) ^c	
ν_3 CH ₂ scissoring	1.0	2158.2	1.0	2104.5	
ν_4 CH ₂ wagging	0.2	1991.9	1.0	2018.6	
	0.2	2078.3			
	0.6	1991.9–2078.3			
ν_5 CH ₂ twisting	0.20	1927.5	1.0	1921.9	
	0.27	1854.5			
	0.53	1854.5–1927.9			
ν_6 CH ₂ rocking	0.31	1598.7	0.20	1524.7	
	0.21	1781.1	0.24	1707.2	
	0.56	1598.7–1784.1	0.56	1524.7–1707.2	
ν_7 C–O stretching	0.22	1333.3	0.22	1385.1	
	0.20	1582.7	0.11	1632.1	
	0.58	1333.3–1582.7	0.67	1385.1–1632.1	
ν_8 C–O stretching	0.41	1310.3	1.0	1304.6	
	0.59	1310.9–1362.1			
B. Skeletal Vibrations					
ν_9 Chain bending	0.10	748.9	1.0	869.7	
	0.17	891.3			
	0.73	748.9–891.3			
ν_{10} Chain torsion and bending	0.06	329.3	0.23	655.0	
	0.29	702.5	0.29	359.7–440.2	
	0.16	266.1–329.3	0.48	359.7–655.0	
	0.49	266.1–702.3			
ν_{11} Chain torsion and bending	0.05	19.4	0.04	156.9	
	0.22	0.1–258.8	0.26	156.9–319.1	
	0.28	129.7–258.8	0.38	129.9–162.3	
	0.45	19.4–129.7	0.32	162.3–319.1	
ν_{12} Chain torsion	0.32	0.1–119.7	1.00	^d	
	0.13	119.7			
	0.34	0.1–119.7			
	0.21	0.1–19.4			

^aData fitted to the dispersion curves of ref. 17.

^bData fitted to the dispersion curves of ref. 16.

^cData not listed in ref. 16, taken identical to those of ref. 17.

^dDispersion curve broken into 90 segments of frequency 0.1 to 138.3 K.

Table 3 Calculated heat capacity at constant volume in J/(k mol of chain atom)

	POM ^a	POMOE ^b	POE ^c	POMO4M ^d	PO3M ^e	PO4M ^f	PO8M ^g	PE ^h
θ_1 (K)	232	317	353	392	433	436	480	519
θ_3 (K)	117	114	114	122	101	91	137	158
A_0 kmol J ⁻¹	3.54E-3	3.90E-3	4.25E-3	4.30E-3	4.40E-3	4.42E-3	4.65E-3	4.85E-3
O/CH ₂	1.0000	0.667	0.500	0.400	0.333	0.250	0.125	0.000
<i>T</i> (K)								
1	0.2040E-3	0.1884E-3	0.1887E-3	0.1587E-3	0.2221E-3	0.2877E-3	0.1279E-3	0.1000E-3
2	0.1632E-2	0.1507E-2	0.1510E-2	0.1270E-2	0.1777E-2	0.2302E-2	0.1023E-2	0.8001E-3
3	0.5508E-2	0.5087E-2	0.5096E-2	0.4286E-2	0.5997E-2	0.7768E-2	0.3452E-2	0.2700E-2
4	0.1306E-1	0.1206E-1	0.1210E-1	0.1016E-1	0.1442E-1	0.1841E-1	0.8183E-2	0.6401E-2
5	0.2550E-1	0.2355E-1	0.2359E-1	0.1984E-1	0.2776E-1	0.3596E-1	0.1598E-1	0.1250E-1
10	0.2027	0.1868	0.1873	0.1580	0.2178	0.2774	0.1277	0.9998E-1
20	0.1268E+1	0.1148E+1	0.1149E+1	0.1020E+1	0.1200E+1	0.1389E+1	0.8868	0.7412
30	0.2690E+1	0.2427E+1	0.2427E+1	0.2243E+1	0.2371E+1	0.2615E+1	0.2095E+1	0.1912E+1
40	0.3949E+1	0.3641E+1	0.3654E+1	0.3450E+1	0.3475E+1	0.3757E+1	0.3349E+1	0.3223E+1
50	0.4959E+1	0.4724E+1	0.4775E+1	0.4574E+1	0.4515E+1	0.4834E+1	0.4540E+1	0.4499E+1
60	0.5764E+1	0.5673E+1	0.5782E+1	0.5607E+1	0.5797E+1	0.5853E+1	0.5659E+1	0.5700E+1
70	0.6428E+1	0.6498E+1	0.6676E+1	0.6544E+1	0.6414E+1	0.6803E+1	0.6697E+1	0.6815E+1
80	0.6998E+1	0.7219E+1	0.7464E+1	0.7383E+1	0.7256E+1	0.7671E+1	0.7648E+1	0.7837E+1
90	0.7505E+1	0.7856E+1	0.8159E+1	0.8131E+1	0.8021E+1	0.8457E+1	0.8509E+1	0.8764E+1
100	0.7970E+1	0.8425E+1	0.8778E+1	0.8799E+1	0.8714E+1	0.9163E+1	0.9284E+1	0.9598E+1
110	0.8407E+1	0.8943E+1	0.9336E+1	0.9400E+1	0.9342E+1	0.9800E+1	0.9981E+1	0.1035E+2
120	0.8826E+1	0.9423E+1	0.9846E+1	0.9948E+1	0.9918E+1	0.1038E+2	0.1061E+2	0.1103E+2
130	0.9233E+1	0.9875E+1	0.1032E+2	0.1046E+2	0.1045E+2	0.1091E+2	0.1119E+2	0.1164E+2
140	0.9634E+1	0.1031E+2	0.1077E+2	0.1093E+2	0.1095E+2	0.1141E+2	0.1173E+2	0.1221E+2
150	0.1003E+2	0.1073E+2	0.1121E+2	0.1139E+2	0.1143E+2	0.1189E+2	0.1224E+2	0.1275E+2
160	0.1043E+2	0.1115E+2	0.1163E+2	0.1183E+2	0.1189E+2	0.1235E+2	0.1273E+2	0.1327E+2
170	0.1083E+2	0.1156E+2	0.1205E+2	0.1227E+2	0.1235E+2	0.1280E+2	0.1320E+2	0.1377E+2
180	0.1123E+2	0.1198E+2	0.1247E+2	0.1271E+2	0.1280E+2	0.1325E+2	0.1368E+2	0.1427E+2
190	0.1164E+2	0.1240E+2	0.1290E+2	0.1315E+2	0.1326E+2	0.1370E+2	0.1416E+2	0.1477E+2
200	0.1206E+2	0.1282E+2	0.1334E+2	0.1360E+2	0.1372E+2	0.1416E+2	0.1464E+2	0.1528E+2
210	0.1248E+2	0.1326E+2	0.1378E+2	0.1405E+2	0.1419E+2	0.1463E+2	0.1514E+2	0.1580E+2
220	0.1292E+2	0.1371E+2	0.1423E+2	0.1452E+2	0.1467E+2	0.1512E+2	0.1564E+2	0.1633E+2
230	0.1336E+2	0.1416E+2	0.1470E+2	0.1500E+2	0.1516E+2	0.1561E+2	0.1616E+2	0.1688E+2
240	0.1380E+2	0.1463E+2	0.1518E+2	0.1549E+2	0.1567E+2	0.1612E+2	0.1670E+2	0.1744E+2
250	0.1426E+2	0.1510E+2	0.1566E+2	0.1599E+2	0.1619E+2	0.1665E+2	0.1725E+2	0.1802E+2
260	0.1472E+2	0.1558E+2	0.1616E+2	0.1651E+2	0.1671E+2	0.1718E+2	0.1781E+2	0.1862E+2
270	0.1519E+2	0.1607E+2	0.1667E+2	0.1703E+2	0.1725E+2	0.1773E+2	0.1839E+2	0.1923E+2
280	0.1566E+2	0.1657E+2	0.1719E+2	0.1756E+2	0.1780E+2	0.1829E+2	0.1898E+2	0.1986E+2
290	0.1613E+2	0.1708E+2	0.1771E+2	0.1810E+2	0.1835E+2	0.1885E+2	0.1958E+2	0.2050E+2
300	0.1661E+2	0.1758E+2	0.1824E+2	0.1865E+2	0.1891E+2	0.1943E+2	0.2019E+2	0.2115E+2
310	0.1709E+2	0.1810E+2	0.1877E+2	0.1920E+2	0.1948E+2	0.2001E+2	0.2080E+2	0.2180E+2
320	0.1757E+2	0.1861E+2	0.1931E+2	0.1975E+2	0.2005E+2	0.2059E+2	0.2142E+2	0.2247E+2
330	0.1805E+2	0.1912E+2	0.1984E+2	0.2031E+2	0.2062E+2	0.2118E+2	0.2205E+2	0.2314E+2
340	0.1853E+2	0.1964E+2	0.2038E+2	0.2087E+2	0.2120E+2	0.2177E+2	0.2268E+2	0.2381E+2
350	0.1901E+2	0.2015E+2	0.2092E+2	0.2143E+2	0.2177E+2	0.2236E+2	0.2331E+2	0.2449E+2
360	0.1948E+2	0.2066E+2	0.2146E+2	0.2199E+2	0.2235E+2	0.2295E+2	0.2394E+2	0.2516E+2
370	0.1995E+2	0.2117E+2	0.2199E+2	0.2254E+2	0.2292E+2	0.2354E+2	0.2456E+2	0.2584E+2
380	0.2042E+2	0.2168E+2	0.2252E+2	0.2309E+2	0.2348E+2	0.2413E+2	0.2519E+2	0.2651E+2
390	0.2088E+2	0.2218E+2	0.2305E+2	0.2364E+2	0.2405E+2	0.2471E+2	0.2581E+2	0.2717E+2
400	0.2134E+2	0.2267E+2	0.2357E+2	0.2418E+2	0.2461E+2	0.2529E+2	0.2642E+2	0.2784E+2
410	0.2179E+2	0.2316E+2	0.2409E+2	0.2472E+2	0.2516E+2	0.2586E+2	0.2707E+2	0.2850E+2
420	0.2223E+2	0.2365E+2	0.2460E+2	0.2525E+2	0.2571E+2	0.2643E+2	0.2764E+2	0.2915E+2
430	0.2267E+2	0.2412E+2	0.2511E+2	0.2577E+2	0.2625E+2	0.2699E+2	0.2824E+2	0.2980E+2
440	0.2310E+2	0.2460E+2	0.2560E+2	0.2629E+2	0.2678E+2	0.2754E+2	0.2883E+2	0.3043E+2
450	0.2352E+2	0.2506E+2	0.2609E+2	0.2680E+2	0.2731E+2	0.2808E+2	0.2941E+2	0.3106E+2
460	0.2394E+2	0.2552E+2	0.2658E+2	0.2731E+2	0.2782E+2	0.2862E+2	0.2999E+2	0.3169E+2
470	0.2435E+2	0.2596E+2	0.2705E+2	0.2780E+2	0.2833E+2	0.2915E+2	0.3056E+2	0.3230E+2
480	0.2475E+2	0.2641E+2	0.2752E+2	0.2829E+2	0.2884E+2	0.2967E+2	0.3112E+2	0.3291E+2
490	0.2515E+2	0.2684E+2	0.2798E+2	0.2877E+2	0.2933E+2	0.3019E+2	0.3167E+2	0.3350E+2
500	0.2554E+2	0.2727E+2	0.2843E+2	0.2924E+2	0.2982E+2	0.3069E+2	0.3221E+2	0.3409E+2

^aPoly(oxyethylene), 2 chain atoms.^bPoly(oxyethyleneoxyethylene), 5 chain atoms.^cPoly(oxyethylene), 3 chain atoms.^dPoly(oxyethyleneoxytetramethylene), 7 chain atoms.^ePoly(oxytrimethylene), 4 chain atoms.^fPoly(oxytetramethylene), 5 chain atoms.^gPoly(oxyoctamethylene), 9 chain atoms.^hPolyethylene, 1 chain atom.

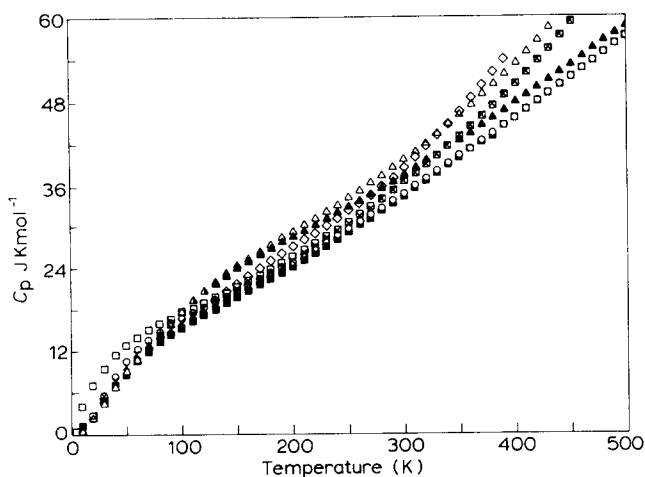


Figure 3 Heat capacity at constant pressure for poly(oxyethylene $(\text{CH}_2\text{-O})_x$). (\diamond) Recommended experimental data. Calculated data using frequencies of Table 2 and the indicated θ temperatures: *Trigonal*: (\square) (no θ -temperatures); (\circ) $N=2$, $\theta_3=122.4$ K, $\theta_1=211.4$ K; (\blacktriangle) $N=4$, $\theta_3=104$ K, $\theta_1=593$ K. *Orthorhombic*: (\blacksquare) (no θ -temperatures); (\times) $N=2$, $\theta_3=232.0$ K, $\theta_1=116.8$ K; (\triangle) $N=4$, $\theta_3=104$ K, $\theta_1=593$ K

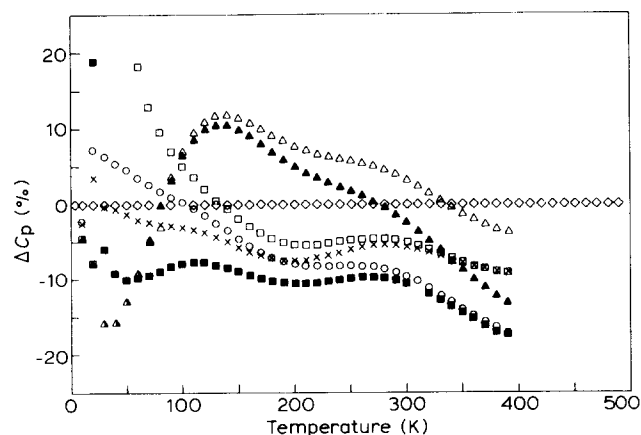


Figure 4 Deviation of the calculated heat capacity C_p from the experimental values. Symbols as in Figure 3

by appropriate averaging so that both columns in Table 2 refer to one $\text{CH}_2\text{-O}$ unit. The experimental heat capacities were, in addition, fitted in several ways to a Tarasov function (equation (5)). First, the skeletal vibrations ν_9 to ν_{12} , $N=4$, were replaced by a θ_3 of 104.0 K and a θ_1 of 593.0 K by fitting between 40 and 200 K⁸. As noted before, this fit shows rather large fluctuations in θ_1 (± 60 K, see also Figure 4). Based on the better frequency spectra listed in Table 2 we repeated the fit for frequencies ν_{11} and ν_{12} only, $N=2$, but using a heat capacity derived by subtracting the calculated heat capacity contributions of ν_1 to ν_{10} . For the trigonal case one finds a θ_3 of 122.4 ± 3.1 K and a θ_1 of 211.4 ± 11 K, and for the orthorhombic case a θ_3 of 116.8 ± 2.9 K and a θ_1 of 232.0 ± 12 K in the temperature range 20 to 60 K. The constant A_0 for the C_v to C_p conversion in equation (6) was found to be 3.54×10^3 (K mol) J^{-1} /chain atom, or 1.77×10^{-3} (K mol) $\text{J}^{-1} \text{mol}^{-1}$ of $\text{CH}_2\text{-O}^{-12}$.

Figure 3 displays the results and Figure 4 the deviations from the experimental recommended data. The full inversion of both spectra to C_p shows a similarly large positive deviation as the calculated polyethylene and

poly(tetrafluoroethylene)⁵ heat capacities. In fact, the trigonal crystal calculations fit at low temperatures (frequencies) even worse than those for the orthorhombic crystal. The orthorhombic Tarasov $N=2$ curve fits perhaps best. As a result, this calculation was used in the subsequent analyses, mainly also because homologous polyoxides with increasing numbers of CH_2 -groups tend towards orthorhombic arrangements. Overall, the agreement between calculation and experiment is somewhat less good than for polyethylene. The chosen curve (\times) has over the 0 to 390 K temperature range (in steps of 10 K) an average deviation of $-5.2 \pm 2.8\%$. This deviation is probably still within the limits of accuracy of the experimental data. In particular, if the measurements on the samples, assumed to be fully crystalline, would contain some portion of amorphous poly(oxyethylene) their heat capacities above about 200 K would be systematically high¹⁸. A comparison of polyethylene and poly(oxyethylene) heat capacities and vibrational spectra reveals that the major differences in heat capacity result from a high chain-bending frequency limit in poly(oxyethylene) (lower C_p of poly(oxyethylene) in the above 100 K region, $\theta_1=593$ K compared to $\theta_1=519$ K of polyethylene), a surprising weaker intermolecular coupling (higher C_p than polyethylene up to 60 K, $\theta_3=104$ K compared to $\theta_3=158$ K of polyethylene), and lower number of C-H bending vibrations (C_p increasingly lagging behind polyethylene above 350 K).

POLY(OXYETHYLENE) POLY(OXYTRIMETHYLENE) AND POLY(OXYTETRAMETHYLENE)

For poly(oxyethylene), poly(oxytrimethylene) and poly(oxytetramethylene) no detailed vibrational frequency analyses are available. Low temperature heat capacity data are, however, available³. The heat capacity of poly(oxytrimethylene) was investigated from 1.4 K to melting (308 K) in 7 overlapping determinations on samples of different crystallinity, permitting, extrapolation to 100% crystallinity. Poly(oxyethylene) heat capacities were measured only on one sample of sufficiently high molecular weight, but of reasonably high crystallinity (0.95) between 90 K and melting (342 K). Poly(oxytetramethylene) [poly(tetrahydrofuran)] heat capacities were measured on three samples of about 0.55 crystallinity between 5 K and melting (330 K). Because of the low crystallinity dependence of the heat capacity below the glass transition temperature (189 K), data up to T_g can be used for analysis.

Rather than using the prior inversions of the heat capacities of these three macromolecules making use of two skeletal vibrations in a Tarasov fit⁸, the experience gained on the poly(oxyethylene) was applied. Tarasov θ_3 and θ_1 values were recalculated using N -values of 4, 6 and 8 for the three respective polymers. In addition, group vibrations of the C-H-bending and stretching, as well as C-C and C-O stretching frequencies have been subtracted before analysis, using the respective frequencies of polyethylene (Table 1, ν_1 - ν_4 and ν_6 - ν_8) and poly(oxyethylene) (Table 2, ν_1 - ν_{10}). The resulting θ_3 and θ_1 values were 113.9 ± 3.7 K, 100.5 ± 2.1 K, 90.0 ± 2.2 K, and 352.8 ± 25 K, 433.2 ± 18 K, 436.1 ± 22 K for poly(oxyethylene), poly(oxytrimethylene), and poly(oxytetramethylene), respectively. The θ -temperatures were

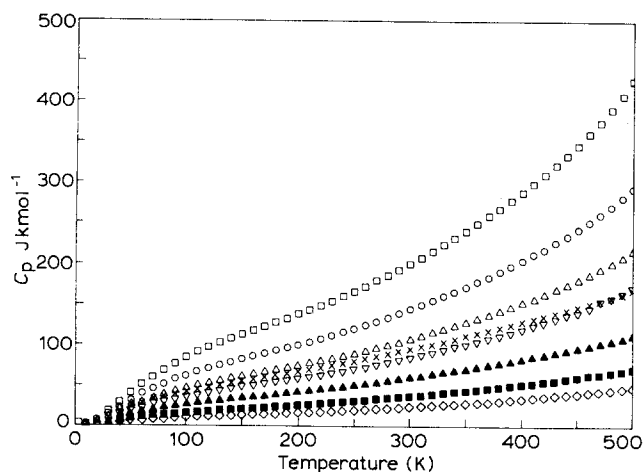


Figure 5 Calculated heat capacities at constant pressure for various polyoxides. Poly(oxyethylene) (▲); poly(oxytrimethylene) (▽); poly(oxytetramethylene) (△). Also shown are poly(oxymethylene) (■); polyethylene (◇); poly(oxymethyleneoxyethylene) (x); poly(oxymethyleneoxytetramethylene) (○); and poly(oxyoctamethylene) (□)

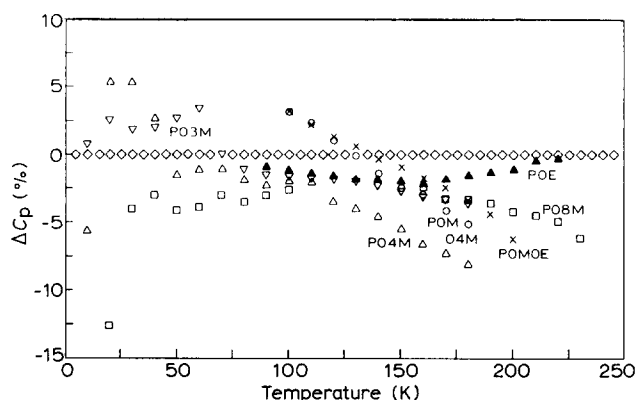


Figure 6 Deviation of the calculated heat capacity C_p from the experimental values. Poly(oxyethylene) (▲); poly(oxytrimethylene) (▽); poly(oxytetramethylene) (△). Also shown are poly(oxymethyleneoxyethylene) (x); poly(oxymethyleneoxytetramethylene) (○) and poly(oxyoctamethylene) (□)

fitted to the heat capacities between 20 and 110 K. Values for A_0 to calculate C_p using equation (6) were 4.25×10^{-3} (K mol) J^{-1} and 4.42×10^{-3} (K mol) J^{-1} /chain atom for poly(oxyethylene) and poly(oxytetramethylene) from experimental fitting at room temperature through equation (5)¹⁰. For poly(oxytrimethylene) A_0 was estimated to be 4.33×10^{-3} (K mol) J^{-1} /mole of chain atom, a reasonable value when considering the slow change of A_0 with composition¹⁰.

Figure 5 shows the results and Figure 6 the deviations from the experimental, recommended data³. Very clearly, experiment and calculation agree within $\pm 5\%$ over the whole temperature range. Eliminating the temperature ranges where measurements were extrapolated to reach low temperatures or to reduce possible residual glass transition effects, the average percentage errors for 10 K steps are $-1.3 \pm 0.6\%$ (90–220 K), $-0.6 \pm 2.3\%$ (10–180 K), and $-3.2 \pm 3.7\%$ (10–180 K) for poly(oxyethylene), poly(oxytrimethylene) and poly(oxytetramethylene), respectively. Based on these results one may conclude that, for the purpose of heat capacity calculation, the frequency spectrum may be approxi-

mated by appropriately weighted addition of poly(oxymethylene) and polyethylene spectra. The skeletal contributions corresponding to the ν_{11} and ν_{12} normal modes of poly(oxymethylene) (Table 2) and ν_5 and ν_9 normal modes of polyethylene (Table 1) must be calculated by the appropriate θ_3 and θ_1 values for the Tarasov expression fitted to the experimental data.

HOMOLOGOUS POLYOXIDES

The remaining questions deal with the possibility of application of the just devised addition scheme of frequencies to homologous polyoxides with less regular O- and CH_2 -sequences and the possibility of prediction of θ_3 and θ_1 as well as A_0 from the fraction of O in the backbone chain. For this purpose we make use of the remaining experimental C_p data on homologous polyoxides of the data bank³. There is one set of high crystallinity (0.91), but low molecular weight data (7000) on poly(oxyoctamethylene), and one investigation each on low molecular weight (2800) and low crystallinity (0.58) poly(oxymethyleneoxyethylene) and on high molecular weight (72000) and low crystallinity (0.50) poly(oxyethyleneoxytetramethylene). The first set of data starts at 13 K, the other two at 90 K. All should correspond reasonably closely to crystalline heat capacities up to the glass transition temperatures 250 K, 209 K and 189 K, respectively. Figure 7 is a plot of all experimentally available A_0 -values for equation 6 as a function of the ratio of O/ CH_2 in the chain. Similarly, Figure 8 is a plot of all θ_3 and θ_1 -values for all polyoxides with measured low temperature heat capacities. Using the appropriately interpolated values of θ_3 and θ_1 as well as A_0 allows the calculation of C_p for all homologous polyoxides. The additional results are also displayed in Figures 5 and 6. The calculated heat capacities correspond again within $\pm 5\%$ to the experimental data, i.e. the use of continuously

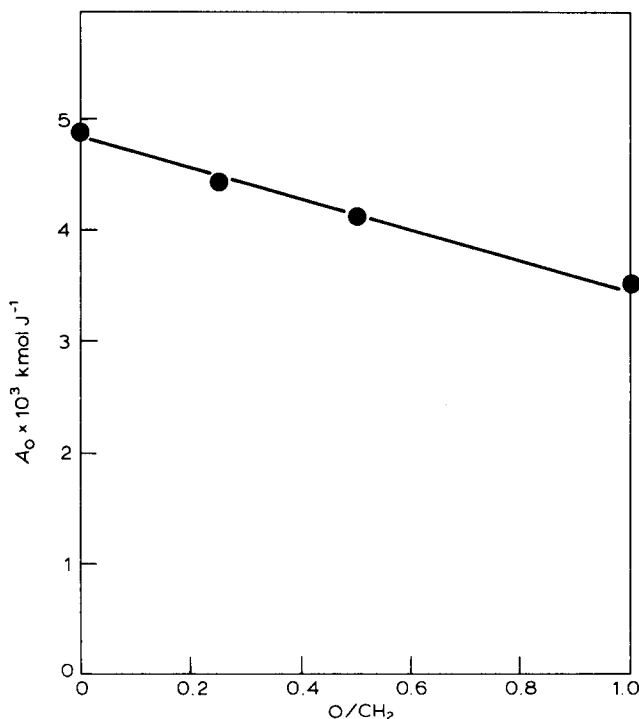


Figure 7 Plot of A_0 per mole of chain atoms as a function of oxygen ratio. [To get A_0 per mole of repeating unit divide by the number of chain atoms]

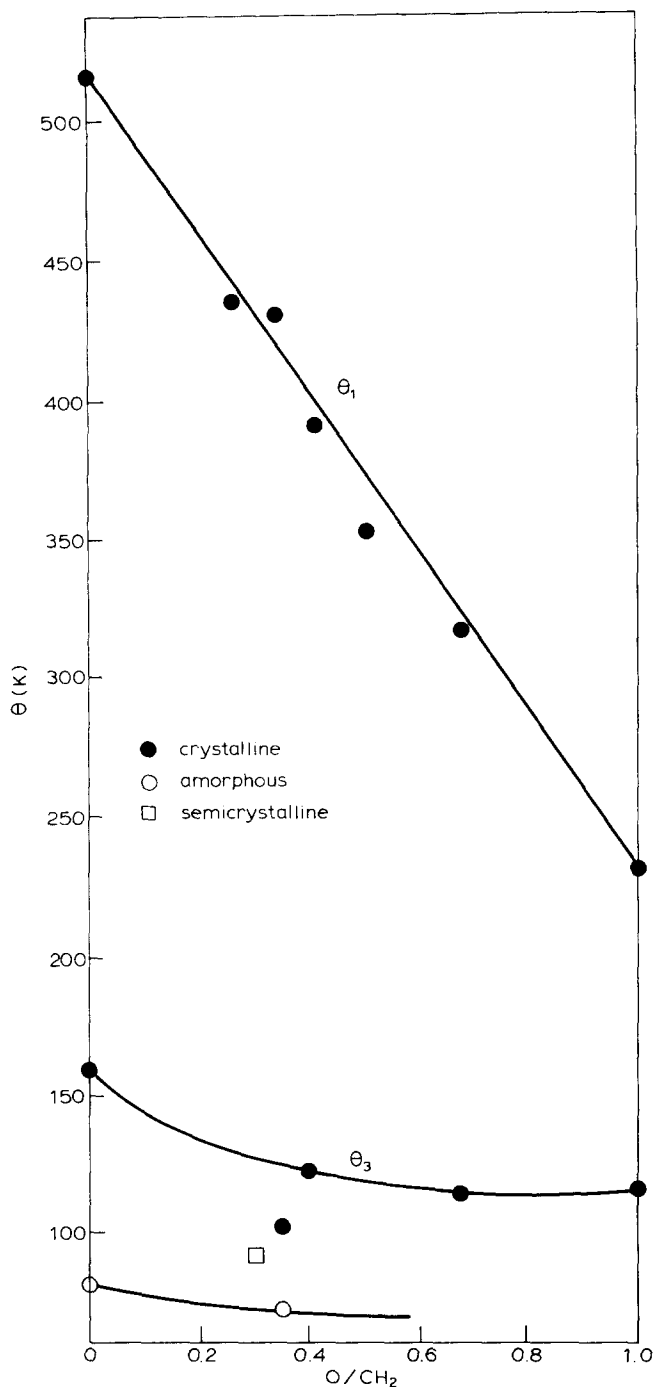


Figure 8 θ_3 and θ_1 for homologous polyoxides as a function of oxygen ratio. [Use equation 5 with $N=2 \times$ number of CH_2 -groups per repeating unit]; (●): crystalline; (○): amorphous; (□): semicrystalline

changing θ_3 , θ_1 and A_0 is a reasonable assumption. Note that the larger deviations in θ_3 may have a reasonable explanation in the limited crystallinity of some of the samples. Note also that A_0 is plotted per mole of chain atoms, i.e. for calculation of C_p per mole of repeating unit, it must be divided by the number of chain atoms.

As a final calculation, Figure 9 is a plot of calculated heat capacities at constant volume for the temperature range up to 1000 K. Table 3 is a list of the corresponding heat capacities.

CONCLUSIONS

An addition scheme for C_p and C_v of crystalline, linear,

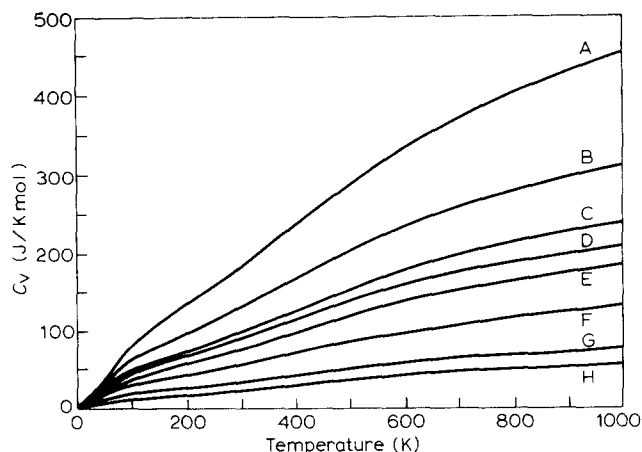


Figure 9 Heat capacity at constant volume for a series of homologous polyoxides. Poly(oxyethylene) (F); poly(oxytrimethylene) (E); poly(oxytetramethylene) (C). Also shown are poly(oxymethylene) (G); poly(ethylene) (H); poly(oxymethyleneoxyethylene) (D); poly(oxymethyleneoxytetramethylene) (B); and poly(oxyoctamethylene) (A)

aliphatic polyoxides from 0 K to melting is developed. The scheme needs for its use the O/CH_2 ratio in the molecule as its only input parameter. Other data are generated automatically from the here presented normal mode and heat capacity discussion (Tables 1 and 2 and curves for the θ -temperature and A_0 variation with O/CH_2 ratio, calculation via equations (1)–(6). Comparison with the extensive experimental data bank shows agreement to $\pm 5\%$ or better. The scheme seems useful for any sequence of O and CH_2 , i.e. for homo as well as copolymers.

The presently available normal mode calculations for crystals of polyethylene and poly(oxymethylene) are in the low frequency, intermolecular vibration region not in agreement with heat capacities. In this region heat capacity is best reproduced by a Tarasov θ_3 , θ_1 expression.

The conversion of the calculated C_v to C_p is accomplished by the well known Nernst–Lindemann expression. Its applicability and limitation to temperatures below melting is discussed elsewhere¹⁰.

The C_v -data in Table 3 may permit the evaluation of other heat capacities by interpolation. Additional data can be generated on request through our ATHAS computation centre (Program CPOXIDES).

ACKNOWLEDGEMENTS

This work has been supported by the Polymers Program of the National Science Foundation, Grant DMR-8317097.

REFERENCES

- 1 Wunderlich, B. *J. Chem. Phys.* 1962, **37**, 1207
- 2 Gaur, U. and Wunderlich, B. *Am. Chem. Soc. Symp. Ser.* 1982, **197**, 355
- 3 Gaur, U., Shu, H.-C., Mehta, A., Lau, S.-F., Wunderlich, B. B. and Wunderlich, B. *J. Phys. Chem. Ref. Data* 1981, **10**, 89, 119, 1001, 1051; 1982, **11**, 313, 1065; 1983, **12**, 29, 65, 91
- 4 Grebowicz, J., Lau, S.-F. and Wunderlich, B. *J. Polym. Sci., Polym. Symp. Edn.* 1984, **72**, 19
- 5 Lau, S.-F. and Wunderlich, B. *J. Polym. Sci., Polym. Phys. Edn.* 1984, **22**, 379

Heat capacities of polyethylene and polyoxides: J. Grebowicz et al.

- 6 Baur, H. and Wunderlich, B. *Adv. Polym. Sci.* 1970, **7**, 151
- 7 Tarasov, V. V. *Zh. Fiz. Khim.* 1950, **24**, 111
- 8 Cheban, Yu. V., Lau, S.-F. and Wunderlich, B. *Colloid Polym. Sci.* 1982, **260**, 9
- 9 Lau, S.-F. and Wunderlich, B. *J. Therm. Anal.* 1983, **28**, 59
- 10 Grebowicz, J. and Wunderlich, B. *Thermal Anal.* to be published 1985
- 11 Barnes, J. and Franconi, B. *J. Phys. Chem. Ref. Data* 1978, **7**, 309
- 12 Arora, R. K. Ph.D. Thesis, University of Delhi (India), 1983, see also ref. 10
- 13 Bares, V. and Wunderlich, B. *J. Polym. Sci. Polym. Phys. Edn.* 1973, **11**, 397
- 14 Tasumi, M., Shimanouchi, T., Miyazawa, T. *J. Mol. Spectrosc.* 1962, **9**, 261; see also Kitagawa, T. and Miyazawa, T. *Adv. Polym. Sci.* 1972, **9**, 335
- 15 Kitagawa, T. and Miyazawa, T. *Rep. Prog. Polym. Phys. Japan* 1966, **9**, 175
- 16 Boeiro, F. J. and Cornell, D. D. *J. Chem. Phys.* 1972, **56**, 1516
- 17 Sugeta, H. Ph.D. Dissertation, Osaka Univ. 1969; see also Kitagawa, T. and Miyazawa, T. *Adv. Polym. Sci.* 1972, **9**, 335
- 18 According to new data on amorphous polyoxymethylene by Suzuki, H., Grebowicz, J. and Wunderlich, B., to be published